Electrochemical characterization of YSZ thick films deposited by dip-coating process

F. Mauvy [a,*], P. Lenormand [b], C. Lalanne [a], F. Ansart [b], J.M. Bassat [a], J.C. Grenier [a],

Groupement de Recherches CNRS "PACTE", GDR 2985

[a] *Institut de Chimie de la Matière Condensée de Bordeaux ICMCB - CNRS, Université Bordeaux 1, 87, av. du Dr. A. Schweitzer, 33 608 Pessac-Cedex, France*

[b] *Centre Interuniversitaire de Recherche et d'Ingénierie et d'Ingénierie des Matériaux, CIRIMAT, Université Paul Sabatier, Bât. 2R1, 118 route de Narbonne, 31062 Toulouse Cedex, France*

Abstract

Yttria stabilized zirconia (YSZ, 8% Y_2O_3) thick films were coated on dense alumina substrates by a dip-coating process. The suspension was obtained by addition of a polymeric matrix in a stable suspension of commercial YSZ (Tosoh) powders dispersed in an azeotropic mixture MEK–EtOH. The suspension composition was improved by the addition of YSZ Tosoh particles encapsulated by zirconium alkoxide sol containing yttrium nitrate which are the precursors of the 8-YSZ oxide. This optimal formulation allowed preparing, via a dip-coating process, thick films which were, after thermal treatment, homogeneous, dense and crack-free. A specific method was performed to measure the electrical conductivity, i.e. to determine the ionic conductivity of the film: it uses the four-point probe technique combined with ac impedance spectroscopy. The good agreement between the classical two-electrode measurements performed on YSZ pellets and the four-electrode ones performed on YSZ films allows concluding that this method is relevant for characterizing the transport properties of thick films.

Keywords: YSZ ionic conductivity; Thick films; Four-point probe conductivity measurements; Sol–gel processes

1. Introduction

Due to the high oxygen-ionic conductivity in both oxidizing and reducing atmospheres, yttria stabilized zirconia (ZrO_2–8% Y_2O_3) is the most commonly used electrolyte material in SOFC technology [1]. Current technological challenges are the control and the optimisation of its microstructure in order to reduce the operating temperature down to 700 °C. Decreasing this temperature generally results in increased voltage losses (internal resistance and electrode over-potential increases). Concerning the ohmic drop through the electrolyte, one possibility to increase the performance at reduced temperatures is to use new types of solid electrolytes with higher oxide ion conductivity (for example doped ceria CGO or lanthanum gallate LSGM [2]). An alternative way is to reduce the electrolyte thickness by using an electrode supported thin film electrolyte. A significant improvement of the cell performances could then be expected.

We report here an original method for synthesizing thick films by using the dip-coating technique [3,4]. A dip-coating solution, similar to those used for the tape casting deposits [5–7], constituted of powders in suspension, is optimized in order to control both the thickness and density of the films. Based on previous works [8], films of about 20 μm thick were prepared on dense polished alumina substrates (insulating material). In order to evaluate the quality of the films, electrical resistivity measurements were performed using a specific experimental set up, the four probe method in an ac mode. The electrical conductivity of these films was compared with that of dense ceramics pellets.

2. Experimental

2.1. Preparation of YSZ thick films

As shown in Fig. 1, the final suspension used in the dip-coating process results from the mixture of an optimized initial

* Corresponding author. Tel.: +33 5 40 00 25 17; fax: +33 5 40 00 83 73.
E-mail address: mauvy@icmcb-bordeaux.cnrs.fr (F. Mauvy).

doi:10.1016/j.jpowsour.2007.06.061

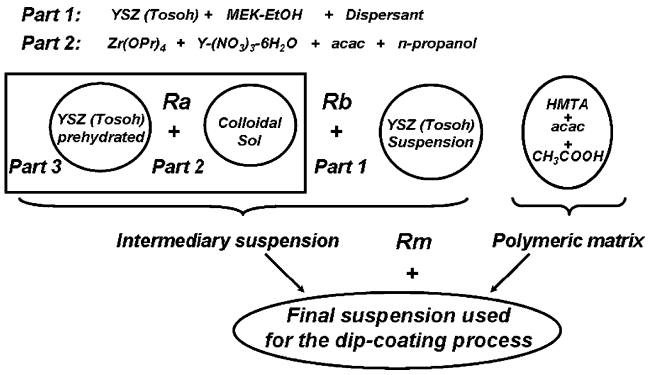

Fig. 1. Flow chart illustrating the processing route for preparing the final suspension used for the dip-coating process.

suspension and a polymeric matrix, the best preparation conditions having been previously reported [9].

First, YSZ commercial powder (Tosoh) was incorporated, under mechanical stirring, in an azeotropic mixture as methylethylketone–ethanol (MEK–EtOH) with a polyesterphosphate (PE-312, CECA S.A.) type-additive used as dispersant [10]. The mass ratio of YSZ powder/MEK–EtOH was controlled and kept equal to 1 (part 1, Fig. 1).

Secondly, colloidal YSZ nanoparticules were synthesized using the alkoxide route [11]. The YSZ precursor sols were prepared starting from a mixture of zirconium *n*-propoxide, *n*-propanol, yttrium nitrate, acetylacetone (acac) and water. Under controlled atmosphere, the zirconium alkoxide was diluted in *n*-propanol and chelated by acetylacetone. The hydrolysis of the complexing ligand is not easy and the control of the chemical reaction could be achieved by avoiding precipitation and slowing down condensation effects. The experimental parameters used for the alkoxide sol preparation were the following: $C = 0.5\,\mathrm{mol\,L^{-1}}$ for the zirconium *n*-propoxide concentration, $R' = [\mathrm{acac}]/\{[\mathrm{ZrO_2}] + [\mathrm{Y_2O_3}]\} = 0.7$ and $W' = [\mathrm{H_2O}]/\{[\mathrm{ZrO_2}] + [\mathrm{Y_2O_3}]\} = 10$ for the complexing and the hydrolysis ratios, respectively. The as-prepared sol was homogeneous, clear and transparent and constituted of very small colloidal particles, YSZ precursors, of about 2–3 nm [11,12].

Thirdly, with the aim to improve the density of the thick films, some YSZ commercial powder was pre-hydrated and added to the alkoxide sol so that the condensation reactions occur on the surface of the oxide particles. With this encapsulating technique [13], the cohesion between the YSZ particles was improved and the density of the layer obtained after thermal treatment increased. Ra was defined as the mass ratio of the pre-hydrated YSZ powder to the alkoxide sol (part 2 + part 3, Fig. 1). Finally, this last mixture was added to the previous YSZ suspension (part 1) in the mass ratio Rb leading to an intermediary suspension.

To this intermediate suspension constituted of the pre-hydrated yttria stabilised zirconia dispersed in the alkoxide sol and of YSZ commercial powder (cf. Fig. 1), a polymeric matrix, derived from the Pecchini process [14], was added. The role of the polymeric matrix is double: to encapsulate YSZ particles in the polymeric chains and to support the adherence of the final suspension on the substrate surface during the dip-coating process. This polymeric matrix was obtained by polymerization and polycondensation reactions between hexamethylenetetramine (HMTA) and acetylacetone in acetic acid medium upon heating. The viscosity, measured at room temperature with a rotating spindle viscosimeter (LAMY-model #TVe-05) and an applied shear rate of $66.5\,\mathrm{s^{-1}}$, was systematically adjusted at about 45 mPa s. Rm was defined as the mass ratio of the polymer matrix to the initial YSZ suspension previously described.

The final suspensions were deposited on dense polycrystalline alumina substrates previously cleaned in successive ultrasonic baths of acetone and alcohol, by the dip-coating technique with a withdrawal speed of about $30\,\mathrm{cm\,min^{-1}}$. The thermal treatment was performed in order to both remove organic compounds and promote a good sintering process. A typical experiment consists in increasing the temperature up to 800 °C with a heating rate of $20\,^\circ\mathrm{C\,h^{-1}}$ and then up to 1400 °C with a heating rate of $100\,^\circ\mathrm{C\,h^{-1}}$, a sintering time of 2 h and finally a slow decreasing temperature down to room temperature.

2.2. Electrical and electrochemical measurements

Ionic conductivity measurements are usually carried out using a classical symmetric two-electrode electrochemical cell. Such geometry cannot be used for thick films because of the small thickness of the electrolytic material and of an asymmetric geometry: this feature led us to find an alternative methodology [15–18].

The electrical resistivity measurements were performed on the as prepared YSZ thick films deposited on alumina substrates. With regard to its highly insulating character, it is supposed in the following that the substrate has no significant contribution to the electrical conductivity. The four-point probe technique with four Pt aligned electrodes was used (Fig. 2a). Four platinum wires were connected to the sample using platinum paste (Ø ≈0.2 mm). The two outer probes were the current-carrying electrodes (I_1, I_2) and the two inner ones (placed 1.5 mm apart) were used for measuring the voltage (E_1, E_2) [18].

For the dc measurements, a Keithley 2400 SourceMeter was used as current generator and a Keithley 199 System DMM/Scanner as voltmeter. The two apparatus were connected to a computer operating under Labview software for conducting the measurements and collecting the data. The applied current intensity was in the range $0 \pm 100\,\mu\mathrm{A}$ (step size: $10\,\mu\mathrm{A}$) provided an ohmic behaviour to be found for the sample.

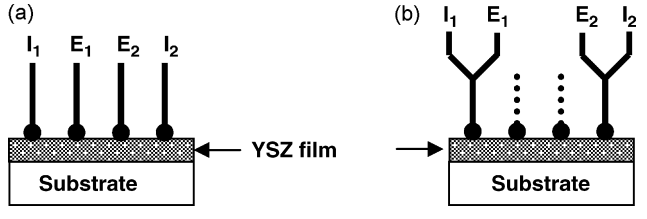

Fig. 2. Scheme of the four-electrode (a) and two-electrode (b) experimental set-up. The probes are equidistant.

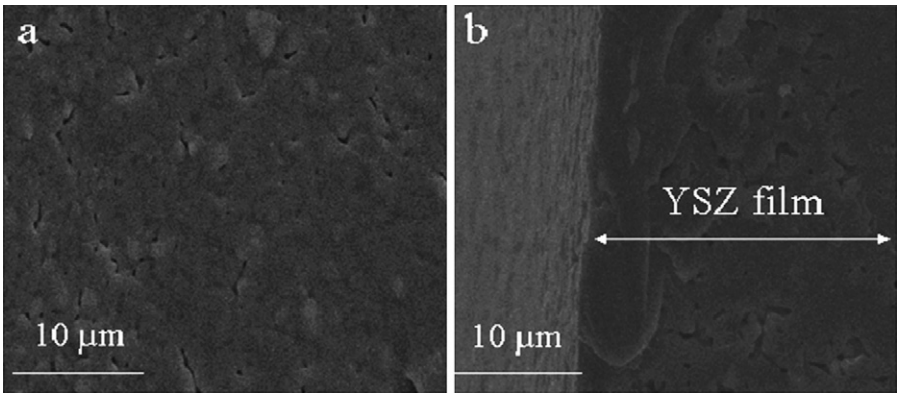

Fig. 3. SEM micrographs of a YSZ thick film obtained by the dip-coating process from a final suspension with Rm = 0.2, Ra = 0.11 and Rb = 0.17 and after annealing at 1400 °C during 2 h: (a) surface and (b) cross-section.

Concerning the ac measurements, the impedance diagrams were obtained with an Ecochemie Autolab in the 0.01–10^6 Hz range with a 50 mV signal amplitude and a 0 mV dc bias. It was checked that in all cases the experimental conditions were in the linear response range of the sample. A curve fitting was performed using the Zview program. Measurements were performed in an air flow (0.06 SLPM), at decreasing temperature from 900 down to 450 °C. For each temperature, the data were collected after annealing times of typically 2 h.

For comparison, some measurements were carried out in ac mode using only the outer electrodes in a two-electrode configuration (Fig. 2b).

3. Results

3.1. Microstructural characterization of thick films

Based on previous studies [8], the experimental parameters for preparing the thick films were as follows: Rm = 0.2, Ra = 0.11 and Rb = 0.17, respectively. As it can be seen in Fig. 3, these layers seem to be relatively dense and no cracks or microcraks can be observed either at the surface or inside the film. Only some micropores are present on the surface. Typically these films were about 25 µm thick.

The YSZ films are well crystallized as evidenced by X-ray diffraction (Fig. 4). EPMA analyses confirm these films to have the expected stoichiometric composition.

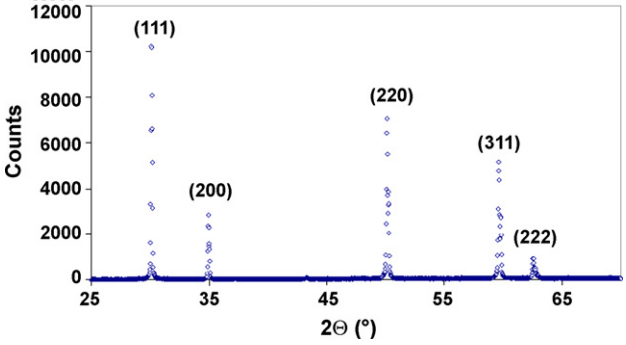

Fig. 4. XRD pattern of the YSZ thick film.

3.2. Conductivity measurements

Firstly, the dc electrical conductivity of the thick films was measured with the four points configuration (co-planar electrodes) versus temperature and under air. Secondly, impedance spectroscopy measurements were performed.

Examples of impedance plots recorded either in a four-electrode or a two-electrode configuration are shown in Figs. 5 and 6, respectively.

All the diagrams of the ac four-electrode configuration (Fig. 5) exhibit similar shapes composed of two depressed semicircles, namely HF (for the high frequency range) and LF (low frequency). The experimental data were well fitted by means of a nonlinear least-square fit using an equivalent circuit composed of a series of two *R*//CPE elements (where *R* is a pure resistance and CPE is a constant phase element $Z_{CPE} = 1/Y_0(j\omega)^p$) [17]. The capacitive effect deduced from the *R* and CPE values is given by:

$$C = R^{(1-p)/p} \times \mathrm{CPE}^{(1/p)} \quad (1)$$

Each semicircle was characterised by a radius *R* (Ω), a relaxation frequency *f* (Hz) and an average capacitance effect *C* (Farads).

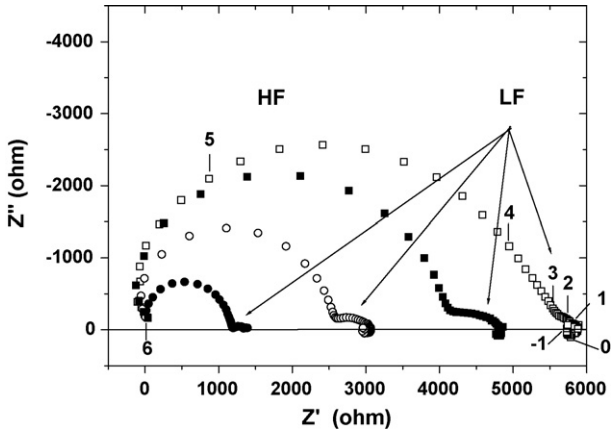

Fig. 5. Typical impedance diagrams recorded with a four-electrode setting: (●) 762 °C; (◯) 712 °C; (■) 662 °C; (□) 611 °C (the numbers indicate the frequency logarithm).

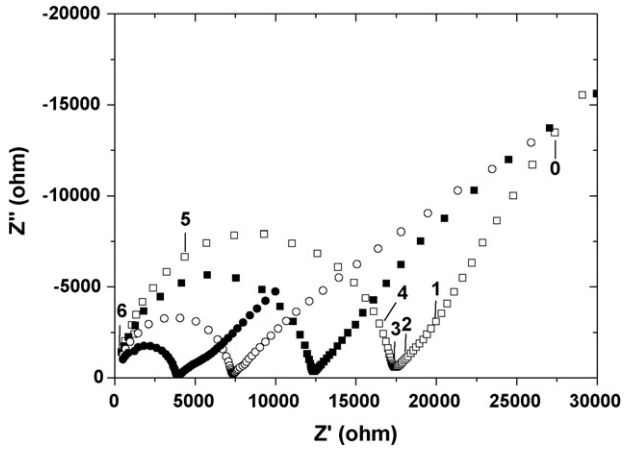

Fig. 6. Typical impedance diagrams recorded with a two-electrode setting: (●) 762 °C; (◯) 712 °C; (■) 662 °C; (□) 611 °C (the numbers indicate the frequency logarithm).

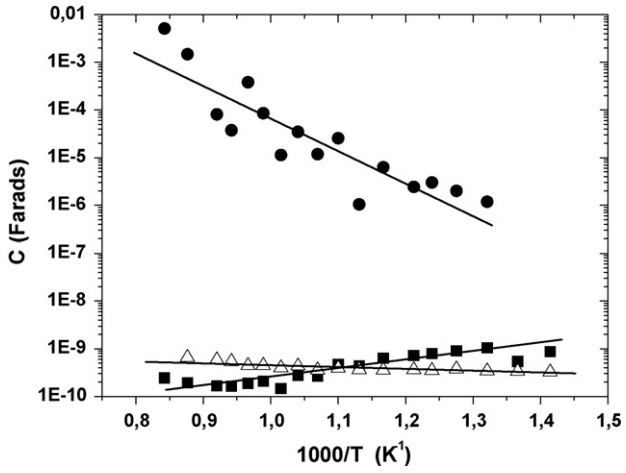

Fig. 7. Arrhenius plots of the CPEs recorded with two- and four-electrode settings: (■) HF four-electrode; (●) LF four-electrode; (△) HF two-electrode.

The conductivity of the deposited layers can be obtained from the relation

$$\sigma = \frac{K}{R} \tag{2}$$

where K is a geometric factor which depends on the size of the sample, on the film thickness and on the distance between electrodes according to the Laplume model [19].

The experimental Nyquist diagrams for the two-electrode configuration (Fig. 6) are composed of one semicircle in the high frequency range and a Warburg-type straight line in the low frequency range. The data were fitted using the equivalent circuit composed of a series of a R//CPE element (high frequency) associated with a Warburg impedance (low frequency range). For the two-electrode geometry, on the basis of the Laplume theory and taking into account that the probes are equidistant, it follows that the K factor is three times that of the four-probe configuration.

From the results of the diagram fits, the interpretation of the physical meaning of CPE elements is usually difficult. As the power parameter p is close to unity, the CPE values can be considered mainly as capacitive effects. With the aim of identifying the various contributions, the CPE values were calculated (in Farad) in the temperature range 900–450 °C and reported in Fig. 7.

The high frequency CPE values are almost constant and rather similar for the two- and four-electrode measurements, about 5×10^{-10} F whereas the LF-CPE values vary from 10^{-6} F at 400 °C to 10^{-2} F at 900 °C [20]. It can be noticed that the p parameter is close to unity for HF contribution whereas p is in the range 0.85–0.95 for LF contribution. The comparison of the measured capacitive effects with data from the literature [19] allows concluding that the high and low frequency contributions can be assigned to the bulk ionic conduction of the YSZ deposited layer and to the electrode process (oxygen reduction), respectively. In our study, the grain boundary impedance contribution is not evidenced.

Therefore, the radius of the HF semicircle R_{HF} was used for calculating the electrical conductivity of the YSZ layer. Its thermal variation ($\log \sigma$ as a function of the reciprocal temperature) is shown in Fig. 8.

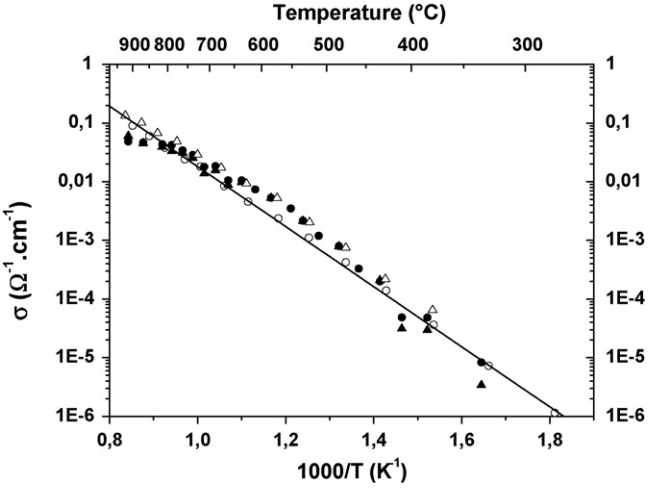

Fig. 8. Arrhenius plots of the electrical conductivity (ac mode) for the YSZ film and pellet: (▲) four-electrode/film; (△) four-electrode/pellet; (●) two-electrode/film; (◯) symmetric two-electrode setting/pellet.

For comparison, a ceramic with a density higher than 95% was prepared from Tosoh powder. Its electrical conductivity was measured using not only a two-electrode symmetrical configuration but also the four-point probe technique in dc and ac mode. Impedance spectroscopy measurements performed on two- and four-electrode cells agree with previously reported data [21,22] and are given in the figure.

The dc measurements of the thick film are plotted in Fig. 9. The dc electrical conductivity of the pellet is also reported for comparison.

4. Discussion

From the data plotted in Fig. 8, one can notice the good agreement for the different ac measurements over the whole temperature range (900–300 °C). Straight lines are observed indicating the Arrhenius-type behaviour, which is consistent

Table 1
Activation energies (eV) of the bulk conductivity for YSZ film and pellet

	Four electrodes/dc	Four electrodes/ac	Two electrodes/ac
Film	$T > 700\,^{\circ}C$; $E_A = 0.96 \pm 0.05$ eV $T < 700\,^{\circ}C$; $E_A = 0.61 \pm 0.05$ eV	$E_A = 0.98 \pm 0.05$ eV	$E_A = 1.01 \pm 0.05$ eV
Pellet	$E_A = 0.95 \pm 0.05$ eV	$E_A = 0.94 \pm 0.05$ eV	$E_A = 1.04 \pm 0.05$ eV

with a classical hopping conduction mechanism. The activation energies are reported in Table 1.

According to these results, the E_A values obtained with the ac technique (two or four electrodes) are close to 1.00 eV, the usual value for the YSZ ionic conductivity [21,22]. One should also point out the good agreement obtained for the electrical conductivity values of the film and of the dense pellet, which allows concluding that the as prepared YSZ films have likely a dense microstructure. It also confirms the relevance of this technique for measuring the ionic conductivity of deposited layers.

It is also important to notice that grain boundary resistance contribution was not found when fitting the impedance spectra [23–25], which corroborates that the films are indeed very dense as observed in the micrographs (Fig. 3). This point is very important with respect to the potential application of this deposition technique in the field of SOFC since high ionic conductivity and low gas permeation are required.

From the above results, one can conclude that the microstructure of the deposited layers exhibits a low porosity: all the conductivity values reported in this work characterize only bulk properties, which reveals this deposition technique to be efficient for preparing dense electrolyte films.

Concerning the dc measurements performed on films, the agreement with ac ones is observed only at high temperatures ($T > 700\,^{\circ}C$) where the ohmic behaviour – i.e. the linearity between the applied current and the measured voltage – is verified. At lower temperatures ($T < 700\,^{\circ}C$), it is no longer observed.

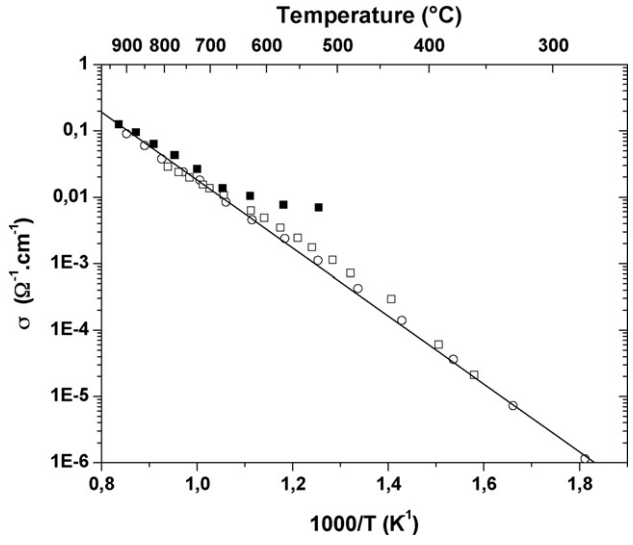

Fig. 9. Arrhenius plots of the electrical conductivity (dc mode) for the YSZ film and pellet: (■) four-electrode/film; (□) four-electrode/pellet; (◯) symmetric two-electrode setting/pellet (ac mode as reported in Fig. 8).

This behaviour may be due to polarisation phenomena (depletion or accumulation of oxygen near the electrodes bringing the current), which results in potential perturbations on electrodes measuring the voltage giving erroneous values of the measured resistance. Thus, the conductivity and activation energies collected at temperatures lower than 700 °C are higher and inconsistent with literature data (cf. Table 1) [21,22]. This phenomenon could be reduced by increasing the distance between the electrodes and the thickness of the film [26].

These observations suggest that this setting of co-planar electrodes under ac conditions is well adapted for measuring high resistances. Nevertheless specific precautions concerning the electrode geometry and the current values are necessary under dc polarisation to prevent polarisation phenomena when resistance becomes higher.

5. Conclusions

YSZ films have been deposited on alumina insulating substrates by sol–gel dip-coating process. X-ray diffraction and EPMA analyses confirm these films to be well crystallised and to have the expected stoichiometric composition. A specific method using the four-point probe technique combined with ac impedance spectroscopy has been performed for measuring their ionic conductivity. The good agreement between the classical two-electrode measurements performed through YSZ pellets and the four-electrode (co-planar electrodes) performed on YSZ films allows concluding that this method can be relevant for characterizing the ionic conductivity of thin films. This point is of a particular interest for SOFC applications provided that dense thick films can be grown on porous anodes.

References

[1] A. Weber, E. Ivers-Tiffee, J. Power Sources 127 (2004) 273–283.
[2] V.V. Kharton, F.M.B. Marques, A. Atkinson, Solid State Ionics 174 (2004) 135–149.
[3] J. Kim, Y.S. Lin, J. Membr. Sci. 139 (1998) 75–83.
[4] X. Changrong, C. Huaqiang, W. Hong, Y. Pinghua, M. Guangyao, P. Dingkun, J. Membr. Sci. 162 (1999) 181–188.
[5] H. Tianmin, L. Zhe, H. Yinglong, G. Pengfei, G. Pengfei, L. Jiang, S. Wenhui, J. Alloys Compd. 337 (2002) 231–236.
[6] F. Snijkers, A. De Wilde, A. Mullens, J. Luyten, J. Eur. Ceram. Soc. 24 (2004) 1107–1110.
[7] A. Mukherjee, B. Maiti, A. Das Sharma, R.N. Basu, H.S. Maiti, Ceram. Int. 27 (2001) 731–739.
[8] M. Gaudon, Ph.D. Thesis, Université P. Sabatier, Toulouse, France, 2002.
[9] P. Lenormand, D. Caravaca, C. Laberty-Robert, F. Ansart, J. Eur. Ceram. Soc. 25 (2005) 2643–2646.
[10] T. Chartier, C. Hinczewski, S. Corbel, J. Eur. Ceram. Soc. 19 (1999) 67–74.
[11] A. Lecomte, A. Dauger, P. Lenormand, J. Appl. Cryst. 33 (2000) 496–499.

[12] P. Lenormand, Ph.D. Thesis, Université de Limoges, France, 2001.
[13] D.C. Bradley, D.G. Carter, Can. J. Chem. 39 (1961) 1434–1443.
[14] P. Pechini, US Patent, 3.330.697.
[15] L.G.J. de Haart, R.A. Kuipers, K.J. de Vries, A.J. Burggraaf, J. Electrochem. Soc. 138 (1991) 1970–1975.
[16] X. Chen, N.J. Wu, A. Ignatiev, J. Eur. Ceram. Soc. 19 (1999) 819–822.
[17] T. Tsai, S.A. Barnett, J. Electrochem. Soc. 142 (1995) 3084–3087.
[18] Y.L. Yang, C.L. Chen, S.Y. Chen, C.W. Chu, A.J. Jacobson, J. Electrochem. Soc. 147 (2000) 4001–4007.
[19] J. Laplume, L'onde électrique 335 (1955) 113.
[20] F. Mauvy, J.M. Bassat, E. Boehm, J.P. Manaud, P. Dordor, J.C. Grenier, Solid State Ionics 158 (2003) 17–28.
[21] M. Mogensen, T. Lindegaard, U.R. Hansen, G. Mogensen, J. Electrochem. Soc. 141 (1994) 2122–2128.
[22] B. Steele, C. R. Acad. Sci. Paris, Série IIc (1998) 533–543.
[23] J. Fleig, J. Maier, Solid State Ionics 94 (1997) 199–207.
[24] J. Fleig, S. Rodewald, J. Maier, Solid State Ionics 136–137 (2000) 905–911.
[25] M. Lang, T. Franco, R. Henne, S. Schaper, G. Schiller, in: A.J. Mc Evoy (Ed.), Proc. 4th European Solid Oxide Fuel Cell Forum, Lucerne, 2000, pp. 231–240.
[26] F. Ménil, V. Coillard, H. Debéda, Cl. Lucat, Sens. Actuators B 77 (2001) 84–89.